Accounting for Acceleration – Signal Parameters Estimation Performance Limits in High Dynamics Applications

4 authors:

Hamish McPhee
Telecommunications for Space and Aeronautics
3 PUBLICATIONS **5** CITATIONS

SEE PROFILE

Lorenzo Ortega Espluga
Institut Polytechnique des Sciences Avancées
43 PUBLICATIONS **127** CITATIONS

SEE PROFILE

Jordi Vilà-Valls
Institut Supérieur de l'Aéronautique et de l'Espace (ISAE)
129 PUBLICATIONS **815** CITATIONS

SEE PROFILE

E. Chaumette
Institut Supérieur de l'Aéronautique et de l'Espace (ISAE)
174 PUBLICATIONS **1,039** CITATIONS

SEE PROFILE

Some of the authors of this publication are also working on these related projects:

Performance bounds for misspecified models View project

Accounting for Acceleration – Signal Parameters Estimation Performance Limits in High Dynamics Applications

Hamish McPhee, Lorenzo Ortega, Jordi Vilà-Valls, *Senior Member, IEEE*, Eric Chaumette, *Member, IEEE*

Abstract—The derivation of estimation lower bounds is paramount to designing and assessing the performance of new estimators. A lot of effort has been devoted to the range-velocity estimation problem, a fundamental stage on several applications, but very few works deal with acceleration, being a key aspect in high dynamics applications. Considering a generic band-limited signal formulation, we derive a new general compact form Cramér-Rao bound (CRB) expression for joint time-delay, Doppler stretch, and acceleration estimation. This generalizes and expands upon known delay/Doppler estimation CRB results for both wideband and narrowband signals. This new formulation, especially easy to use, is created based on baseband signal samples, making it valid for a variety of remote sensors. The new CRB expressions are illustrated and validated with representative GPS L1 C/A and Linear Frequency Modulated (LFM) chirp band-limited signals. The mean square error (MSE) of a misspecified estimator (conventional delay/Doppler) is compared with the derived bound. The comparison indicates that for some acceleration ranges the misspecified estimator outperforms a well specified estimator that accounts for acceleration.

Index Terms—Cramér-Rao bound, delay/Doppler/acceleration estimation, signal parameter estimation, band-limited signals, maximum likelihood, GNSS, radar.

I. INTRODUCTION

RANGE and velocity estimation appear in a plethora of applications such as navigation, radar, or remote sensing, being a key stage of the receiver [1]–[4]. In addition, phase estimation can be instrumental in precise Global Navigation Satellite Systems (GNSS) navigation [3], which is directly linked to the underlying delay/Doppler estimation. Tracking of some complicated systems may require compensation of Doppler variation over time. An example of such systems is seen in the micro-Doppler effect investigated by [5] for vibrating targets. In high dynamics scenarios, acceleration of the target similarly causes an additional shift in the Doppler frequency. Traditional delay/Doppler synchronization may not be enough to achieve a good performance in these scenarios. This performance degradation also impacts carrier phase-based applications. Although a lot of effort has been devoted to range-velocity (i.e., delay/Doppler) estimation, very few works deal with acceleration, which may be fundamental when localizing, tracking, or positioning highly dynamic targets/vehicles.

The main goal of this contribution is to obtain meaningful insights on the estimation performance under high dynamics, correctly accounting for acceleration. The ideal performance in the mean square error (MSE) sense is given by the Cramér-Rao lower bound (CRB) [6], which gives an accurate MSE estimation of the maximum likelihood estimator (MLE) in the asymptotic region, i.e., the large sample and/or high signal-to-noise (SNR) regimes of the Gaussian conditional signal model (CSM) [7], [8].

Several CRB expressions have been derived for the delay, Doppler, and phase estimation under the narrowband signal assumption [1], [9]–[13], but in some applications, the compression or stretch on the envelope of the received signal cannot be ignored [14]. The latter has been analyzed for the wideband range/Doppler MLE and its associated ambiguity function [15]–[17]. The derivations of CRBs under the wideband signal assumption have received fewer attention [18]–[23]. The limitations of the wideband range/velocity CRBs in the literature have been recently overcome in [24], leading to a general compact CRB expression for amplitude, phase, delay, and Doppler stretch estimation. It is sensible to expect that acceleration plays an important role in several high dynamics applications. Yet a compact CRB in the vein of [10], [24] including delay, Doppler, and acceleration estimation, for a generic band-limited signal, is not available in the literature. This prevents analysis of the impact of acceleration on estimation performance in the asymptotic region. On the one hand, in certain applications, adding acceleration estimation in the first receiver stage may improve the overall performance, e.g., targets with highly varying Doppler. On the other hand, adding a parameter to be estimated almost always leads to CRBs higher than those found in [10], [24] for delay/Doppler estimation. This leaves a chance that the performance of an MLE converging to the newly derived CRB could be worse than the performance found for delay/Doppler MLEs, which assume a zero acceleration. From a theoretical perspective [25], neglecting acceleration results in a mismatched model (a.k.a. misspecified model) of the signal and a mismatched delay/Doppler estimator. Therefore, the performance of the mismatched/misspecified estimation is used as a comparison to conclude whether including acceleration estimation should be preferred.

The main contributions of this article are: i) extend the recent narrowband CRB results in [10], to include acceleration; ii) extend the recent wideband CRB results in [24], to include acceleration. In both cases several new terms appear

which can not be guessed from existing expressions in the literature; iii) application of proposed CRBs for assessing the performance obtained through the use of optimal delay/Doppler/acceleration estimation in high dynamic scenarios; and iv) assess the performance of the misspecified delay/Doppler estimator to determine regions of operation where the new bound represents the preferred estimator (the high dynamics region). The new theoretical results are validated for two representative scenarios: GPS L1 C/A and Linear Frequency Modulated (LFM) chirp band-limited signals.

It is worth pointing out that there exist some inherent differences between both GNSS and radar applications. While radar systems may not be coupled with other sensors and therefore the analysis provided in this article brings new insights on the overall system performance, in the GNSS case it is common practice to have additional aiding sensors, i.e., such as inertial navigation systems (INS) [3, Ch. 28], if the receiver is expected to suffer high dynamics. Indeed, GNSS/INS coupling [26] was proposed to address high dynamics situations, and more specifically ultra-tight architectures where the INS is used to steer the GNSS receiver tracking loops, reducing the parameter dynamics that such loops have to track. Another alternative is the use of high-order tracking loops able to lock to rapidly varying synchronization parameters. Despite these alternatives available in the GNSS literature, the theoretical tools derived in this article bring meaningful insights: i) on the impact of high dynamics at the GNSS acquisition stage (e.g., re-acquisition), ii) in the case of extended integration schemes, high-sensitivity receivers [27, Ch. 18] or GNSS reflectometry [28], where the apparent acceleration may be much larger than under nominal conditions, iii) to provide an initial performance characterization of high-order tracking loops (i.e., high-order sequential maximum likelihood estimators), and iv) for the design of low cost receivers and/or small platforms not able to integrate navigation grade INS.

Notation: Scalar values are defined in italic (a), vector in bold lower-case ($\mathbf{a}$), and matrices bold upper-case ($\mathbf{A}$). $||\mathbf{x}|| = \sqrt{\sum x_i^2}$ is the L2 norm of vector $\mathbf{x}$ with i elements and $|x|$ gives the absolute value of the scalar x. The transpose operation is indicated by the superscript ^{T}, the conjugate transpose by the superscript ^{H}, and the conjugate operation by the superscript *. $\mathbf{I}_n$ represents the identity matrix of dimension n, $Re\{\cdot\}$ and $Im\{\cdot\}$ refer to the real part and the imaginary part. The rectangular unit step function is represented by: $1_{\left[-\frac{B}{2}, \frac{B}{2}\right]}(f)$ limited by bandwidth B.

II. SIGNAL MODEL

The parameters being estimated are linked to the positioning of a moving target, so the variables linked to position and motion should be defined. The vectors $\mathbf{p}$, $\mathbf{v}$, $\mathbf{a}$ are defined for the instantaneous position, velocity, and acceleration, respectively, all relative to the origin of a Reference Frame (the Earth Centered Reference Frame for instance in GNSS).

To define the estimation problem of interest, consider the line-of-sight (LOS) transmission of a band-limited signal $s(t)$ (bandwidth B) with sampling frequency F_s over a carrier with frequency f_c (wavelength $\lambda_c = c/f_c$), from a transmitter T at
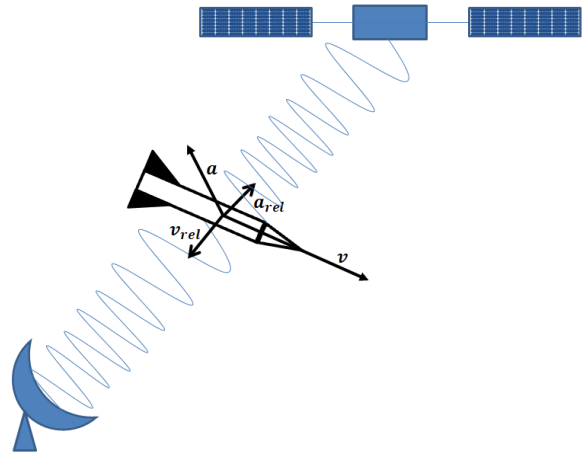

Fig. 1. The relative, line-of-sight acceleration and velocity that contribute to the Doppler effect, and the specific parameters that can be estimated.

position $\mathbf{p}_T(t) = \mathbf{p}_T(0) + \mathbf{v}_T t + \frac{1}{2}\mathbf{a}_T t^2$ to a receiver R at position $\mathbf{p}_R(t) = \mathbf{p}_R(0) + \mathbf{v}_R t + \frac{1}{2}\mathbf{a}_R t^2$. Note the initial position being used here is a reference point for a general derivation of how the acceleration effects the signal model, in the true tracking case, the terms $\mathbf{p}_T(0)$ and $\mathbf{p}_T(0)$ should be replaced with the previous known (or estimated) positions throughout the tracking loop. The standard baseband signal with bandwidth related to the sampling frequency by $B \leq F_s$, can be expressed in time and frequency as,

$$s(t) = \sum_{k=-N_1'}^{N_2'} s\left(\frac{k}{F_s}\right) \text{sinc}\left(\pi F_s\left(t - \frac{k}{F_s}\right)\right) \rightleftharpoons \qquad (1a)$$

$$s(f) = \frac{1}{F_s} \sum_{k=-N_1'}^{N_2'} s\left(\frac{k}{F_s}\right) e^{-j2\pi\frac{k}{F_s}} \times 1_{\left[-\frac{B}{2}, \frac{B}{2}\right]}(f) \qquad (1b)$$

where $\rightleftharpoons$ refers to the Fourier transform to the frequency domain, and N_1', $N_2' \in \mathbb{Z}$, as these values approach infinity the equations give an exact representation of the analog signal in a discretized formulation. Now the signal defined in equation (1a) takes some time (τ) to arrive at the receiver after being transmitted. This delay is the first parameter to be estimated, varying over time and depending on the LOS motion between the transmitter and receiver to give a function of time for the actual delay $\tau_A(t)$. The usual assumption of zero acceleration gives a dependence only on the Doppler ($\tau_A(t) = \tau + bt$); this work will show how a non-zero acceleration is included for our investigation. The radial displacement between transmitter and receiver is proportional to the transmitter to receiver signal time-delay, which is affected by the relative motion between both transmitter and receiver. In high dynamics receivers, in addition to the Doppler effect, we take into account the relative acceleration. Figure 1 below indicates the appropriate components of the target's velocity and acceleration that cause the shifting of the signal. In this case, the receiver can be on the target itself as is the case for GNSS tracking or at the ground radar. The components $\mathbf{v}_{rel}$ and $\mathbf{a}_{rel}$ represent the radial components relative to the signal source. They are projections of the target's actual dynamics ($\mathbf{v}$, $\mathbf{a}$) onto the LOS vector between transmitter and receiver. We define τ as the

initial absolute delay between signal transmission and receival for a perfectly stationary transmitter and target, neglecting additional propagation delay due to the atmosphere. The ideal, actual time between transmission and receival is then shifted only according to the Doppler and acceleration over a certain time, given by (3). This develops from the equation which describes the distance traveled by the transmitted signal

$$\mathbf{p}_{TR} \triangleq \|\mathbf{p}_T (t - \tau_A (t)) - \mathbf{p}_R (t)\| = c\tau_A (t; \boldsymbol{\eta})$$

$$\simeq \|\mathbf{p}_T (0) - \mathbf{p}_R (0)\| + \mathbf{v}_{rel} t + \frac{\mathbf{a}_{rel} t^2}{2}, \qquad (2)$$

with $\tau_A (t; \boldsymbol{\eta}) \simeq \tau + bt + dt^2$,

$$\tau = \frac{\|\mathbf{p}_T (0) - \mathbf{p}_R (0)\|}{c}, b = \frac{\|\mathbf{v}_{rel}\|}{c}, d = \frac{\|\mathbf{a}_{rel}\|}{2c} \qquad (3)$$

that is, a second-order approximation, with c the speed of light. The set of scalar parameters is $\boldsymbol{\eta} = [\tau, b, d]^T$, each term being considered as constant over the duration of the observation period. This is representative of performing an estimation of the parameters at an instantaneous, initial state in time, i.e. an acquisition $\tau = \tau_A(0), b = b_0$ and $d = d_0$. The performance of estimation for this acquisition is a good baseline for the analysis of including acceleration estimation in general cases as they can be represented by consecutive estimations of the instantaneous parameters.

The complex analytic signal at the antenna output is then a function of the actual delay and modulated by the carrier wave, which is also shifted through multiplication with the Doppler and acceleration parameters.

$$x_A(t) = \alpha_A e^{-j2\pi f_c (t - \tau_A(t;\boldsymbol{\eta}))} s (t - \tau_A(t;\boldsymbol{\eta})) + n_A(t), \qquad (4)$$

with $n_A(t)$ a zero-mean white complex circular Gaussian noise, and α_A an amplitude factor that depends on the signal power, polarisation vectors, and antenna gains [29].

In contrast to the standard narrowband signal assumption [1], [9]–[13], where the Doppler effect on the baseband signal is not considered and amounts to a frequency shift, i.e., $s(t - \tau_A(t)) \simeq s(t - \tau)$, we consider the wideband assumption with both delay and dilatation into the baseband signal model, $s(t - \tau_A(t)) \simeq s((1 - b)(t - \tau))$. The expression in (4) is simplified through IQ demodulation in the receiver that uses a Hilbert filter. For short observation times, a good approximation of the Hilbert filter output is found in [30] leading to the simplified model of the carrier's shift due to delay, Doppler, and acceleration in equation (6),

$$x (t) = x_A (t) e^{-j2\pi f_c t} = \alpha a(t; \boldsymbol{\eta}) + n (t), \qquad (5)$$

$$a(t; \boldsymbol{\eta}) = e^{-j2\pi f_c (b(t-\tau)+d(t-\tau)^2)} s ((1 - b)(t - \tau)), \quad (6)$$

with $f \in \left[-\frac{F_s}{2}, \frac{F_s}{2}\right]$, $\frac{F_s}{2} \geq \max_b \left\{\frac{B}{2}(1 - b)\right\}$, $n(t)$ a complex white circular Gaussian noise within this bandwidth with unknown variance σ_n^2, and $\alpha = \alpha_A e^{-j2\pi f_c \tau(1+b+d\tau)}$. Propagation time-delay and Doppler dilation effects are detailed by:

$$s (t; \boldsymbol{\eta}) = s ((1 - b)(t - \tau)) \rightleftharpoons s (f; \boldsymbol{\eta}) \quad = \frac{1}{1 - b} s \left(\frac{f}{1 - b}\right) e^{-j2\pi}$$

The discrete vector signal model is built from $N = N_1 + N_2 + 1$ ($N_1/F_s \gg N_1'/B$, $N_2/F_s \gg N_2'B$) samples at $T_s = 1/F_s$,

$$\mathbf{x} = \alpha \mathbf{a}(\boldsymbol{\eta}) + \mathbf{n} = \rho e^{j\varphi} \mathbf{a}(\boldsymbol{\eta}) + \mathbf{n}, \qquad (7)$$

$$\mathbf{x} = [\ldots, x (kT_s), \ldots]^\top, \mathbf{n} = [\ldots, n (kT_s), \ldots]^\top,$$

$$\mathbf{s} = [\ldots, s (kT_s), \ldots]^\top,$$

$$\mathbf{a}(\boldsymbol{\eta}) = [\ldots, s((1 - b)(kT_s - \tau))e^{-j2\pi f_c (b(kT_s-\tau)+d(kT_s-\tau)^2)}, \ldots]^\top,$$

with $N_1 \leq k \leq N_2$ and $\mathbf{n} \sim \mathcal{CN}\left(\mathbf{0}, \sigma_n^2 \mathbf{I}_N\right)$. The unknown deterministic parameters can be gathered in vector $\boldsymbol{\epsilon} = \left[\sigma_n^2, \rho, \varphi, \tau, b, d\right]^\top$, with $\alpha = \rho e^{j\varphi}$ ($\rho \in \mathbb{R}^+$, $0 \leq \varphi \leq 2\pi$). In this contribution a single LOS transmission is considered, however, (7) can also be obtained if one considers transmission via diffraction or reflection [29], [31] and for multiple signal sources.

III. BACKGROUND ON MLE AND AMBIGUITY FUNCTION

Considering (7), the MLE that provides the estimated values of the delay, Doppler, and acceleration is calculated using a correlation between the received signal with noise ($\mathbf{x}$) and a number of simulated replica signals without noise [2], [32]. The vector of estimated parameters $\widehat{\boldsymbol{\eta}} = [\widehat{\tau}, \widehat{b}, \widehat{d}]$ is defined as[1], [2], [32],

$$\widehat{\boldsymbol{\eta}} = \arg\min_{\boldsymbol{\eta}} \left\{\mathbf{x}^H \mathbf{\Pi}_{\mathbf{a}(\boldsymbol{\eta})}^\perp \mathbf{x}\right\} = \arg\max_{\boldsymbol{\eta}} \left\{\frac{|\mathbf{a}(\boldsymbol{\eta})^H \mathbf{x}|^2}{\mathbf{a}(\boldsymbol{\eta})^H \mathbf{a}(\boldsymbol{\eta})}\right\}. \qquad (8)$$

Varying the parameters of interest in (8) within a span of potential solutions within $\pm 3\sigma$ deviation from the true value, where σ^2 is a diagonal element of the derived CRB, allows to check the newly derived CRBs. Indeed, the MSE of MLEs (8) must approach the derived CRB under high SNR conditions [8]. The maximum SNR at the output of the MLE matched filter including compensation for the wideband signal model is $\text{SNR}_{\text{out}} = \frac{|\alpha|^2 \mathbb{E}}{(\sigma_n^2/F_s)(1-b)}$ [23], with $\mathbb{E} = \int_{-\infty}^{+\infty} |s (t)|^2 dt$ the signal energy. The corresponding ambiguity function is defined in [29], also being valuable in the comparison with the derived CRB. For a range of potential values of the estimated parameters $\boldsymbol{\eta}^0$, the ambiguity is maximum and indicates optimum error with the values of $\mathbf{a}(\boldsymbol{\eta} = \boldsymbol{\eta}^0)$. For values of $\boldsymbol{\eta}^0$ different to $\boldsymbol{\eta}$, the ambiguity function decreases,

$$\Xi\left(\boldsymbol{\eta}; \boldsymbol{\eta}^0\right) = \frac{|\alpha|^2}{N} \left\|\mathbf{a}\left(\boldsymbol{\eta}^0\right)\right\|^2 \left|\frac{\mathbf{a}(\boldsymbol{\eta})^H \mathbf{a}(\boldsymbol{\eta}^0)}{\|\mathbf{a}(\boldsymbol{\eta})\| \|\mathbf{a}(\boldsymbol{\eta}^0)\|}\right|^2. \qquad (9)$$

The ambiguity function can be approximated by a 2nd order Taylor expansion, which includes a matrix defined in the derivation of the Fisher Information Matrix (FIM), $\mathbf{\Phi}(\boldsymbol{\eta})$ [10],

$$\Xi (\boldsymbol{\eta} + d\boldsymbol{\eta}; \boldsymbol{\eta}) \simeq \frac{|\alpha|^2}{N} \|\mathbf{a}(\boldsymbol{\eta})\|^2 \left(1 - \frac{1}{2} d\boldsymbol{\eta}^T \left(\frac{2\text{Re}\{\mathbf{\Phi}(\boldsymbol{\eta})\}}{\|\mathbf{a}(\boldsymbol{\eta})\|^2}\right) d\boldsymbol{\eta}\right), \qquad (10)$$

---

[1]Let $S = span(\mathbf{A})$ be the linear span of the set of the column vectors of matrix $\mathbf{A}$, $\mathbf{\Pi}_{\mathbf{A}} = \mathbf{A} \left(\mathbf{A}^H \mathbf{A}\right)^{-1} \mathbf{A}^H$ is the orthogonal projection over S, and $\mathbf{\Pi}_{\mathbf{A}}^\perp = \mathbf{I} - \mathbf{\Pi}_{\mathbf{A}}$.

where the second term, which depends on $\mathbf{\Phi}(\boldsymbol{\eta})$ is directly related to the CRB (17),

$$\mathbf{\Phi}(\boldsymbol{\eta}) = \frac{\partial \mathbf{a}(\boldsymbol{\eta})}{\partial \boldsymbol{\eta}^T}^H \mathbf{\Pi}_{\mathbf{a}(\boldsymbol{\eta})}^{\perp} \frac{\partial \mathbf{a}(\boldsymbol{\eta})}{\partial \boldsymbol{\eta}^T} = \left\| \frac{\partial \mathbf{a}(\boldsymbol{\eta})}{\partial \boldsymbol{\eta}^T} \right\|^2 - \frac{\left| \mathbf{a}(\boldsymbol{\eta})^H \frac{\partial \mathbf{a}(\boldsymbol{\eta})}{\partial \boldsymbol{\eta}^T} \right|^2}{\|\mathbf{a}(\boldsymbol{\eta})\|^2}. \tag{11}$$

Both the MLE and ambiguity function are instrumental to validate the CRB expressions derived in this contribution (refer to Section V).

It is worth pointing out that the amplitude and phase MLEs are given by the magnitude and argument of the cross-ambiguity function, respectively evaluated at the delay, Doppler and acceleration MLEs [32],

$$\widehat{\varphi}(\widehat{\boldsymbol{\eta}}) = \arg \left\{ \left(\mathbf{a}^H(\widehat{\boldsymbol{\eta}}) \mathbf{a}(\widehat{\boldsymbol{\eta}}) \right)^{-1} \mathbf{a}^H(\widehat{\boldsymbol{\eta}}) \mathbf{x} \right\} \tag{12}$$

$$\widehat{\rho}(\widehat{\boldsymbol{\eta}}) = \left| \left(\mathbf{a}^H(\widehat{\boldsymbol{\eta}}) \mathbf{a}(\widehat{\boldsymbol{\eta}}) \right)^{-1} \mathbf{a}^H(\widehat{\boldsymbol{\eta}}) \mathbf{x} \right| \tag{13}$$

If the delay/Doppler/acceleration MLE reaches its asymptotic performance then so do the amplitude and phase estimates. This clearly shows that not correctly accounting for the acceleration can also impact amplitude and phase estimates. The MLE of the noise variance is not stated because it has a trivial equation found in [32].

IV. NEW COMPACT CRB FOR JOINT TIME-DELAY, DOPPLER STRETCH AND ACCELERATION ESTIMATION

A. Background

Considering that the parameters to be estimated are $\boldsymbol{\epsilon} = \left[\sigma_n^2, \rho, \varphi, \tau, b, d \right]^\top$, we recall that [10], $CRB_{\sigma_n^2} = \frac{1}{N} \left(\sigma_n^2 \right)^2$ and

$$CRB_\rho = \frac{\sigma_n^2}{2 \|\mathbf{a}(\boldsymbol{\eta})\|^2}$$
$$+ \rho^2 \frac{\text{Re} \left\{ \mathbf{a}^H(\boldsymbol{\eta}) \frac{\partial \mathbf{a}(\boldsymbol{\eta})}{\partial \boldsymbol{\eta}^\top} \right\} \mathbf{CRB}_\eta \, \text{Re} \left\{ \mathbf{a}^H(\boldsymbol{\eta}) \frac{\partial \mathbf{a}(\boldsymbol{\eta})}{\partial \boldsymbol{\eta}^\top} \right\}^\top}{\|\mathbf{a}(\boldsymbol{\eta})\|^4}, \tag{14}$$

$$CRB_\varphi = \frac{\sigma_n^2}{2\rho^2} \frac{1}{\|\mathbf{a}(\boldsymbol{\eta})\|^2}$$
$$+ \frac{\text{Im} \left\{ \mathbf{a}^H(\boldsymbol{\eta}) \frac{\partial \mathbf{a}(\boldsymbol{\eta})}{\partial \boldsymbol{\eta}^\top} \right\} \mathbf{CRB}_\eta \, \text{Im} \left\{ \mathbf{a}^H(\boldsymbol{\eta}) \frac{\partial \mathbf{a}(\boldsymbol{\eta})}{\partial \boldsymbol{\eta}^\top} \right\}^\top}{\|\mathbf{a}(\boldsymbol{\eta})\|^4}, \tag{15}$$

$$\mathbf{CRB}_{\eta,\varphi} = -\mathbf{CRB}_\eta \frac{\text{Im} \left\{ \mathbf{a}^H(\boldsymbol{\eta}) \frac{\partial \mathbf{a}(\boldsymbol{\eta})}{\partial \boldsymbol{\eta}^\top} \right\}^\top}{\|\mathbf{a}(\boldsymbol{\eta})\|^2}. \tag{16}$$

Then, concerning the recent narrowband/wideband results in [10], [24], we need to compute the CRB of $\boldsymbol{\eta}$ for the Gaussian CSM accounting for the acceleration in (7), which is given by [2],

$$\mathbf{CRB}_\eta = \frac{\sigma_n^2}{2|\alpha|^2} \text{Re} \left\{ \mathbf{\Phi}(\boldsymbol{\eta}) \right\}^{-1}, \tag{17}$$

---

[2] Please note that in some cases where the parameters are not of the same order, the inverse of the FIM cannot be calculated without numerical inaccuracies. In that case, it is required to normalize the parameters, such that they are of the same order to guarantee a numerically stable calculation of the inverse of the FIM.

with $\mathbf{\Phi}(\boldsymbol{\eta})$ defined in (11), allowing easy computation of the CRB through simple matrix substitutions as well as the terms $\mathbf{a}^H(\boldsymbol{\eta}) \frac{\partial \mathbf{a}(\boldsymbol{\eta})}{\partial \boldsymbol{\eta}^\top}$ and $\|\mathbf{a}(\boldsymbol{\eta})\|^2$ to update CRB_ρ, CRB_φ and $\mathbf{CRB}_{\eta,\varphi}$.

B. New Compact form $\mathbf{CRB}_\eta$ Expression

Let us define $\beta = 1 - b$ and $\omega_c = 2\pi f_c$. Then, we aim to derive a compact formulation of $\text{Re} \left\{ \mathbf{\Phi}(\boldsymbol{\eta}) \right\}$, which can be rewritten as

$$\text{Re} \left\{ \mathbf{\Phi}(\boldsymbol{\eta}) \right\} = \begin{bmatrix} (\cdot)_{1,1} & (\cdot)_{1,2} & (\cdot)_{1,3} \\ (\cdot)_{1,2} & (\cdot)_{2,2} & (\cdot)_{2,3} \\ (\cdot)_{1,3} & (\cdot)_{2,3} & (\cdot)_{3,3} \end{bmatrix} \tag{18}$$

$$= \text{Re} \left\{ \frac{\partial \mathbf{a}(\boldsymbol{\eta})}{\partial \boldsymbol{\eta}^T}^H \frac{\partial \mathbf{a}(\boldsymbol{\eta})}{\partial \boldsymbol{\eta}^T} \right\}$$

$$- \text{Re} \left\{ -\frac{1}{\|\mathbf{a}(\boldsymbol{\eta})\|^2} \left(\mathbf{a}(\boldsymbol{\eta})^H \frac{\partial \mathbf{a}(\boldsymbol{\eta})}{\partial \boldsymbol{\eta}^T} \right)^H \left(\mathbf{a}(\boldsymbol{\eta})^H \frac{\partial \mathbf{a}(\boldsymbol{\eta})}{\partial \boldsymbol{\eta}^T} \right) \right\}.$$

After tedious calculus (refer to Appendix A for details), the terms in $\text{Re} \left\{ \mathbf{\Phi}(\boldsymbol{\eta}) \right\}$ are given by the following (with several new terms w.r.t. the delay/Doppler case [24])

$$(\cdot)_{1,1} = F_s \left(\begin{array}{c} \beta^2 \left(W_{3,3} - \frac{|w_3|^2}{w_1} \right) + 4\omega_c^2 d^2 \left(W_{2,2} - \frac{|w_2|^2}{w_1} \right) \\ -4\omega_c d\beta \text{Im} \left\{ W_{3,2} - \frac{w_2^* w_3}{w_1} \right\} \end{array} \right),$$

$$(\cdot)_{1,2} = F_s \left(\begin{array}{c} 2\omega_c^2 d \left(\frac{|w_2|^2}{w_1} - W_{2,2} \right) \\ -\omega_c \beta \text{Im} \left\{ \frac{w_2^* w_3}{w_1} - W_{3,2} \right\} \\ -\omega_c \beta \text{Im} \left\{ \frac{w_5^* w_2}{w_1} - W_{5,2}^* \right\} \\ -\beta \text{Re} \left\{ \frac{w_5^* w_3}{w_1} - W_{5,3}^* \right\} \end{array} \right),$$

$$(\cdot)_{1,3} = F_s \left(\begin{array}{c} 2\omega_c^2 d \left(\frac{w_2 w_4^*}{w_1} - W_{4,2}^* \right) \\ -\omega_c \beta \text{Im} \left\{ \frac{w_4^* w_3}{w_1} - W_{4,3}^* \right\} \end{array} \right),$$

$$(\cdot)_{2,2} = F_s \left(\begin{array}{c} \omega_c^2 \left(W_{2,2} - \frac{|w_2|^2}{w_1} \right) + \left(W_{5,5} - \frac{|w_5|^2}{w_1} \right) \\ +2\omega_c \text{Im} \left\{ W_{5,2} - \frac{w_2 w_5}{w_1} \right\} \end{array} \right),$$

$$(\cdot)_{2,3} = F_s \left(\omega_c^2 \left(W_{4,2}^* - \frac{w_2 w_4^*}{w_1} \right) - \omega_c \text{Im} \left\{ \frac{w_5 w_4^*}{w_1} - W_{5,4} \right\} \right),$$

$$(\cdot)_{3,3} = F_s \omega_c^2 \left(W_{4,4} - \frac{|w_4|^2}{w_1} \right), \tag{19}$$

and the terms $w_1, \ldots, w_5, W_{2,2}, \ldots, W_{5,5}$ are computed by exploiting the properties of a band-limited signal as

$$w_1 = \frac{1}{\beta F_s} \mathbf{s}^H \mathbf{s}, \quad w_2 = \frac{1}{\beta^2 F_s^2} \mathbf{s}^H \mathbf{D} \mathbf{s}, \quad w_3 = \frac{1}{\beta} \mathbf{s}^H \mathbf{\Lambda} \mathbf{s},$$

$$w_4 = W_{2,2} = \frac{1}{\beta^3 F_s^3} \mathbf{s}^H \mathbf{D}^2 \mathbf{s}, \quad w_5 = W_{3,2} = \frac{1}{\beta^2 F_s} \mathbf{s}^H \mathbf{D} \mathbf{\Lambda} \mathbf{s},$$

$$W_{3,3} = \frac{F_s}{\beta} \mathbf{s}^H \mathbf{V} \mathbf{s}, \quad W_{4,2} = \frac{1}{\beta^4 F_s^4} \mathbf{s}^H \mathbf{D}^3 \mathbf{s},$$

$$W_{4,3} = W_{5,2} = \frac{1}{\beta^3 F_s^2} \left(\mathbf{s}^H \mathbf{D} \mathbf{\Lambda} \mathbf{D} \mathbf{s} - \mathbf{s}^H \mathbf{D} \mathbf{s} \right),$$

$$W_{4,4} = \frac{1}{\beta^5 F_s^5} \mathbf{s}^H \mathbf{D}^4 \mathbf{s},$$

$$W_{5,3} = \frac{1}{\beta^2} \left(\mathbf{s}^H \mathbf{\Lambda} \mathbf{s} + \mathbf{s}^H \mathbf{V} \mathbf{D} \mathbf{s} \right),$$

$$W_{5,4} = \frac{1}{\beta^4 F_s^3}\left(\mathbf{s}^H \mathbf{D}\mathbf{\Lambda}\mathbf{D}^2\mathbf{s} - \mathbf{s}^H\mathbf{D}^2\mathbf{s}\right),$$

$$W_{5,5} = \frac{1}{\beta^3 F_s}\left(\mathbf{s}^H\mathbf{s} + \mathbf{s}^H\mathbf{D}\mathbf{V}\mathbf{D}\mathbf{s} - 2\mathrm{Re}\left\{\mathbf{s}^H\mathbf{\Lambda}\mathbf{D}\mathbf{s}\right\}\right), \quad (20)$$

with $\mathbf{D}$, $\mathbf{V}$ and $\mathbf{\Lambda}$ defined as

$$\mathbf{D} = \mathrm{diag}\left([N_1, \; N_1+1, \ldots, \; N_2-1, \; N_2]\right), \quad (21)$$

$$(\mathbf{V})_{n,n'} = \begin{vmatrix} n' \neq n : (-1)^{|n-n'|}\frac{2}{(n-n')^2} \\ n' = n : \frac{\pi^2}{3} \end{vmatrix}, \quad (22)$$

$$(\mathbf{\Lambda})_{n,n'} = \begin{vmatrix} n' \neq n : \frac{(-1)^{|n-n'|}}{(n-n')} \\ n' = n : 0 \end{vmatrix}, \quad (23)$$

for $N_1 \leq n, n' \leq N_2$. It is worth noting that $\mathrm{Re}\left\{\mathbf{\Phi}(\boldsymbol{\eta})\right\}$, and therefore the corresponding CRB depend on the Doppler and acceleration parameters (i.e., b and d). Therefore, for large velocity and acceleration values, it is expected that the CRB cannot neglect these terms when assessing the asymptotic estimation precision of τ and b. Due to the magnitude of the parameters themselves being of low order, it is unclear exactly how much of a difference the typical values for high dynamics applications can impact the CRB until the final value for CRB is computed.

Injecting the corresponding $w_1, \ldots, w_5, W_{2,2}, \ldots, W_{5,5}$ from (20) into (19), and inverting $\mathrm{Re}\left\{\mathbf{\Phi}(\boldsymbol{\eta})\right\}$ leads to a new compact form CRB expression, which has been derived using baseband signal samples. To complete these results and obtain the missing amplitude and phase CRB expressions in (14) and (15), we have by the same integral equations for $\mathbf{w}$ and $\mathbf{Qw}$ (Appendix A): $\|\mathbf{a}(\boldsymbol{\eta})\|^2 = F_s w_1 = \frac{\mathbf{s}^H\mathbf{s}}{\beta}$ and

$$\mathbf{a}(\boldsymbol{\eta})^H \frac{\partial \mathbf{a}(\boldsymbol{\eta})}{\partial \boldsymbol{\eta}^T} = F_s \mathbf{s}^H \mathbf{s}\begin{pmatrix} j\frac{\omega_c}{\beta F_s}(1-\beta) - \frac{\mathbf{s}^H\mathbf{\Lambda}\mathbf{s}}{\mathbf{s}^H\mathbf{s}} \\ -j\frac{\omega_c(1-2d)}{\beta^2 F_s^2}\frac{\mathbf{s}^H\mathbf{D}\mathbf{s}}{\mathbf{s}^H\mathbf{s}} - \frac{1}{\beta^2 F_s}\frac{\mathbf{s}^H\mathbf{D}\mathbf{\Lambda}\mathbf{s}}{\mathbf{s}^H\mathbf{s}} \\ -j\frac{\omega_c}{\beta^3 F_s^3}\frac{\mathbf{s}^H\mathbf{D}^2\mathbf{s}}{\mathbf{s}^H\mathbf{s}} \end{pmatrix}^{\top}. \quad (24)$$

These compact form expressions generalize the recent results as in [24] for the joint delay/Doppler estimation, and update the results related to the amplitude and phase CRBs.

C. Special Case: Standard Narrowband Signal Model

Under the standard narrowband signal assumption, i.e., where no Doppler impact is considered on the baseband signal, $s(t - \tau_0(t)) \simeq s(t - \tau)$, $a(t; \boldsymbol{\eta})$ can be rewritten as $a(t; \boldsymbol{\eta}) = e^{-j2\pi f_c(b(t-\tau)+d(t-\tau)^2)} s(t-\tau)$. In this case, the compact form expression of $\mathrm{Re}\left\{\mathbf{\Phi}(\boldsymbol{\eta})\right\}$ simplifies to

$$(\cdot)_{1,1} = F_s\begin{pmatrix} W_{3,3} - \frac{|w_3|^2}{w_1} + 4\omega_c^2 d^2\left(W_{2,2} - \frac{|w_2|^2}{w_1}\right) \\ -4\omega_c d\,\mathrm{Im}\left\{W_{3,2} - \frac{w_2^* w_3}{w_1}\right\} \end{pmatrix},$$

$$(\cdot)_{1,2} = F_s\left(2\omega_c^2 d\left(\frac{|w_2|^2}{w_1} - W_{2,2}\right) - \omega_c\,\mathrm{Im}\left\{\frac{w_2^* w_3}{w_1} - W_{3,2}\right\}\right),$$

$$(\cdot)_{1,3} = F_s\left(2\omega_c^2 d\left(\frac{w_2 w_4^*}{w_1} - W_{4,2}^*\right) - \omega_c\,\mathrm{Im}\left\{\frac{w_4^* w_3}{w_1} - W_{4,3}^*\right\}\right),$$

$$(\cdot)_{2,2} = F_s\left(\omega_c^2\left(W_{2,2} - \frac{|w_2|^2}{w_1}\right)\right),$$

$$(\cdot)_{2,3} = F_s\left(\omega_c^2\left(W_{4,2}^* - \frac{w_2 w_4^*}{w_1}\right)\right),$$

$$(\cdot)_{3,3} = F_s\left(\omega_c^2\left(W_{4,4} - \frac{|w_4|^2}{w_1}\right)\right), \quad (25)$$

and

$$\mathbf{a}(\boldsymbol{\eta})^H \frac{\partial \mathbf{a}(\boldsymbol{\eta})}{\partial \boldsymbol{\eta}^T} = F_s \mathbf{s}^H \mathbf{s}\begin{pmatrix} j\frac{\omega_c}{\beta F_s}(1-\beta) - \frac{\mathbf{s}^H\mathbf{\Lambda}\mathbf{s}}{\mathbf{s}^H\mathbf{s}} \\ -j\frac{\omega_c(1-2d)}{\beta^2 F_s^2}\frac{\mathbf{s}^H\mathbf{D}\mathbf{s}}{\mathbf{s}^H\mathbf{s}} - j\frac{\omega_c}{\beta^3 F_s^3}\frac{\mathbf{s}^H\mathbf{D}^2\mathbf{s}}{\mathbf{s}^H\mathbf{s}} \end{pmatrix}^{\top}. \quad (26)$$

These expressions generalize the recent narrowband delay/Doppler estimation results in [10], and the corresponding amplitude and phase CRB expressions computation. Finally, for the main parameters of interest, the CRBs can be simply taken from $\mathbf{CRB}_{\boldsymbol{\eta}}$:

$$\begin{aligned} CRB_\tau &= \mathbf{CRB}_{\boldsymbol{\eta}}(1,1), \quad CRB_b = \mathbf{CRB}_{\boldsymbol{\eta}}(2,2), \\ CRB_d &= \mathbf{CRB}_{\boldsymbol{\eta}}(3,3). \end{aligned} \quad (27)$$

V. VALIDATION AND DISCUSSION

A. GPS L1 C/A Signal Scenario

To assess the validity of the new CRB expressions we consider first a GPS L1 C/A band-limited signal. The so-called Pseudo-Random Noise (PRN) code has a length of 1023 chips with a chip rate of 1.023 MHz. We consider a signal duration of 10 ms (i.e., 10 consecutive PRN codes) and $F_s = 2.046$ MHz. To synthesize a high dynamics scenario we consider a Doppler equal to 10 kHz and acceleration equal to 100g (g= 9.81 m/s^2), this being a representative case for instance in an anti-ballistic missile.

First, we assess if the ambiguity function (9) and its 2nd order Taylor approximation (10) coincide. In that perspective, we consider a scenario where only the acceleration parameter d is to be estimated. This result is illustrated in Figure 2, with a clear fit between the ambiguity function and its approximation for a wide range of acceleration values. This is the first proof of the exactness of the CRB, but the complete estimation problem still needs to be characterized.
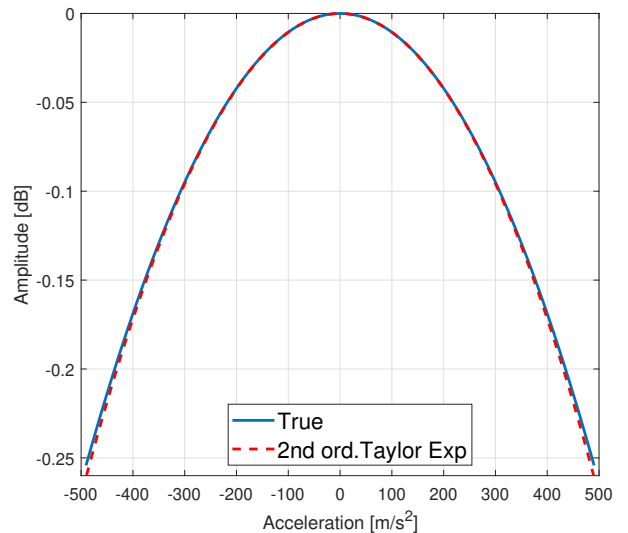

Fig. 2. Ambiguity function and 2nd order Taylor approximation for the acceleration estimation with a GPS L1 C/A band-limited signal.

Since (7) belongs to the class of CSM [7], the MLE converges to the CRB at high SNR [8], a property which can be used as an alternative way to confirm the CRB validity, as previously mentioned. Then, a second experiment is carried out with the signal model in (6) and 10 ms of signal, with $\boldsymbol{\eta} = [\tau, b, d]^{\top}$ unknown deterministic parameters to be estimated. The new CRBs and the corresponding MLEs (8), in terms of SNR_{out} are obtained for 1000 Monte Carlo runs and shown in Figure 3. The MLE converges to the CRB for each parameter, which confirms the validity and exactness of the CRBs. In the following subsection, we will discuss further results about the estimation of the delay, Doppler, and acceleration parameters. In the corresponding analysis, the cases of using a well-specified model and a misspecified/mismatched model have been compared for estimation performance. Any case where the misspecified estimator performs better than the derived CRB including acceleration indicates that the bound does not truly represent the preferred estimator, i.e., the well-specified estimator is overfitting by including joint acceleration estimation.

Mismatch estimation performance

To assess the effect of acceleration on the estimation of delay, Doppler, and acceleration, the delay/Doppler MLE, termed "mismatch", is compared to the joint delay/Doppler/acceleration MLE and the corresponding CRB. Since the mismatched MLE is only performing the simultaneous estimation of two parameters and neglecting acceleration (assuming $d = 0$), the performance will be closer to that seen in [24]; however, the effects of acceleration on the carrier propagation and the evolution of Doppler are not accounted for in that work. The MSE obtained by the mismatch MLE can be expected to deviate from the previously derived CRB. This may imply overall worse performance for the mismatch MLE compared to the delay/Doppler/acceleration MLE, due to the presence of acceleration. The CRB_b (27) for the latter case is seen to have increased because of the additional estimation effort, a sign of overfitting. First, we can see in Figure 4 (top) that the delay estimation is not affected by an acceleration of 100 g for a duration of 10 ms: both MLE τ_0 and MLE τ_0 "Mismatch" coincide. This is a result which shows that the addition of acceleration estimation does not have a negative or positive effect for short enough estimation periods. What is more illustrative on the impact of acceleration is the effects for a longer estimation interval of 20 ms, where the acceleration has more time to take effect and shift the true value from the estimated mismatch value. Figure 4 also shows the results of the mismatched delay estimation for 20 ms and accelerations ranging up to 100 g. The conclusion from [24] that the delay CRB is decoupled from the Doppler still holds, and the same is true for decoupling from acceleration in our derivation. The acceleration effectively increases the SNR threshold, that is the SNR required for the mismatch MLE performance to converge to the CRB at high SNR regime. Figure 4 shows that the MLE including acceleration outperforms the convergence to the CRB with respect to the mismatched MLE, regardless of acceleration magnitude. Neglecting estimation of a high
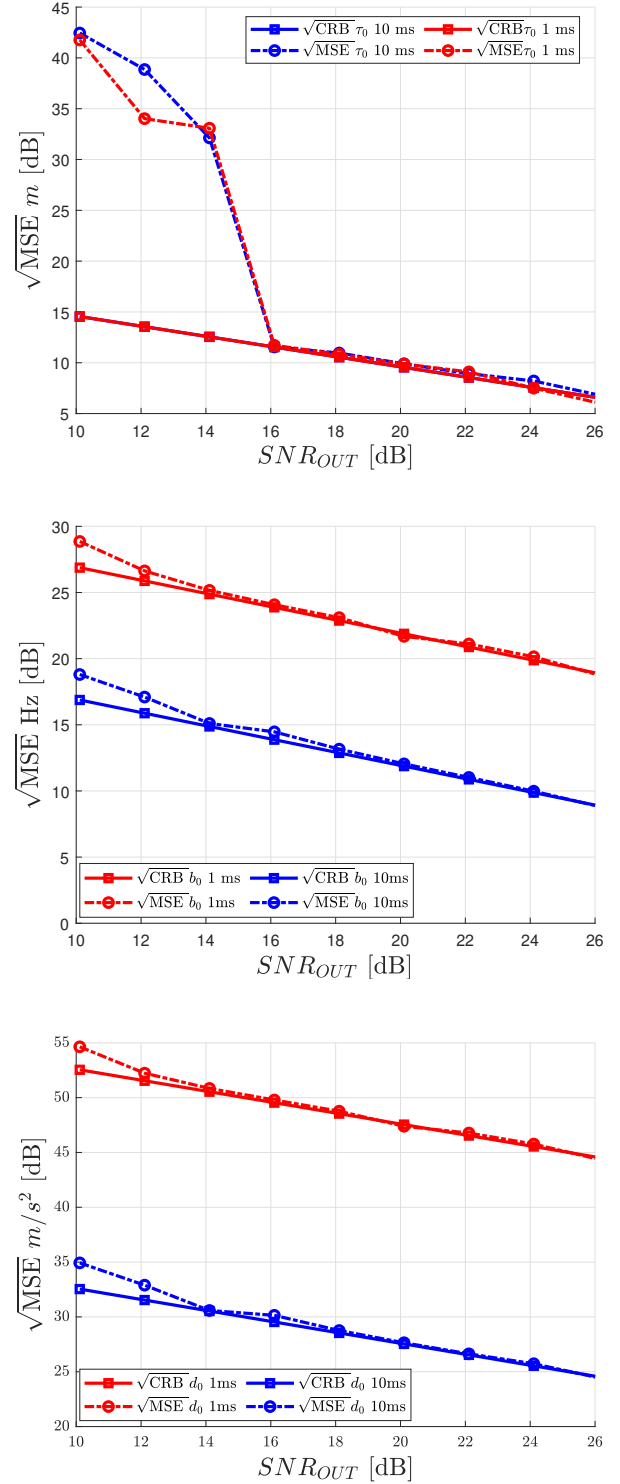

Fig. 3. Delay CRB/MSE for F_s = 2.046 MHz, 1 ms and 10 ms of GPS C/A signal (top). Doppler CRB/MSE for F_s = 2.046 MHz, 1 ms and 10 ms of GPS C/A signal (middle). Acceleration CRB/MSE for F_s = 2.046 MHz, 1 ms and 10 ms of GPS C/A signal (bottom).

magnitude acceleration contributes a virtual noise but does not impact the optimum estimation error for high enough SNR. Therefore, even with long estimation periods, the optimum performance of the mismatched MLE will always coincide with the fully specified MLE at SNR≥ 26 dB. This is also an important result for low SNR applications that can also experience significant acceleration (e.g. ascent vehicles from the moon, large thrust maneuvers to change satellite orbits). Future applications of GNSS for spacecraft positioning can experience low signal quality and hence, need to include the estimation of acceleration to avoid the virtual noise included in the mismatch MLE.
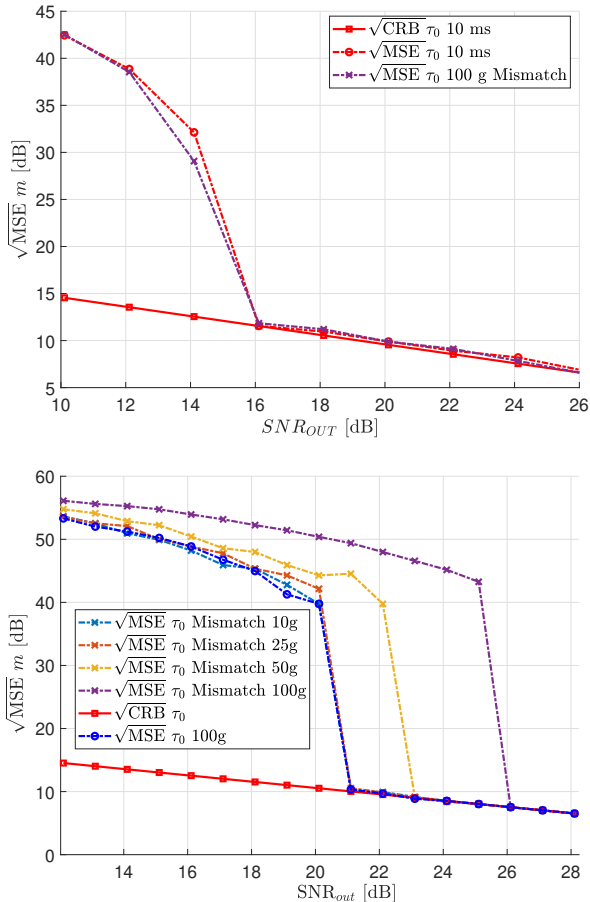

Fig. 4. Delay CRB and MSE mismatch for 10 ms F_s = 2.046 MHz (top) and 20 ms F_s = 1.023 MHz (bottom).

In Figure 5 we show the results for the misspecified Doppler estimation. "CRB_{b_1} without d" refers to the Doppler CRB obtained from the delay/Doppler formulation [24], and "CRB_{b_0}" stands for the new Doppler CRB accounting for acceleration (27). In the first case (zero acceleration), we can see that the Doppler estimate converges to the corresponding CRB without acceleration. This is because the constant Doppler assumption is not broken. Note that the estimation performance is degraded by adding an extra parameter and it is illustrated by the difference between "CRB_{b_0}" and "CRB_{b_1} without d" (6 dB increase). It is noteworthy that the mismatched Doppler estimator performs better than the correctly specified

one for certain SNR values, magnitudes of acceleration, and observation times. This is a clear example of the trade-off between the overfitting induced by an additional parameter and the degradation in MSE expected from a misspecified MLE, which is a theoretical problem that can be tackled by considering the so-called misspecified CRB (MCRB) [25] as exemplified hereinafter.For 10 ms or greater of signal, the acceleration impact on the mismatched MLE is clear. While the MSE accounting for acceleration converges to the CRB, the mismatched Doppler MSE converges to a different value.

Since the derivation of closed-form misspecified CRBs is out of the scope of the present paper (and is left for future work), for the sake of analysis, we resort to numerical computations of the "misspecified CRB" (MCRB) from [33, Eq.(10), Eq.(43), Eq.(44)]. Indeed, the MSE of the misspecified estimator must approach $\sqrt{MCRB + \Delta b^2}$, where Δb gives the difference between the expected value of Doppler with and without acceleration. The same behavior is seen, where the mismatch error approaches a constant value in the asymptotic regime, suggesting a biased estimate. For some acceleration values, the steady value of the MSE crosses the upper CRB including d, giving a threshold where the mismatch estimator performs worse than the fully specified delay/Doppler/acceleration estimation. Figure 5 includes observation intervals of 10 ms (top) and 20 ms (bottom), each of them having a different performance depending on the acceleration. The SNR at which the fully specified estimator performs best is the lowest for higher accelerations. For an observation duration of 20 ms, the high acceleration mismatch cases have a noticeable bias and perform worse than the fully specified CRB at all reasonable SNR values. This is expected for the longer observation period because the Doppler is going to vary significantly over that time interval, proportional to the acceleration. The mismatch MLE fails to account for that and gives a biased estimate. A period of 20 ms is desired for GPS signal acquisition and tracking to achieve the lowest magnitude of error while remaining within the limits of coherent integration. The results of this work show that for observation durations of 10 ms or more, the inclusion of acceleration estimation is necessary for optimum performance of Doppler estimation when targets have high dynamics.

Now, to indicate the point that the target is considered to be under "high dynamics", Figure 6 defines an approximate acceleration threshold for when the mismatched MLE performs worse than the CRB including acceleration. This shows the operational point where ignoring the acceleration term causes that the mismatch MLE perfoms worse than the well-specified MLE. Therefore, the high dynamics region that benefits from acceleration estimation is reached. The performance w.r.t. acceleration is analyzed at a representative SNR of 25 dB, to match real-world applications as well as ensure the error has converged to its steady value.

The Doppler CRB derived in this work does not vary according to the acceleration, but it was shown that the mismatch MLE performance is impacted by significant accelerations. Figure 6 gives a good comparison of the performance for the different times of the signal, with lower MSE for longer time intervals. For a 1 ms observation time, the acceleration is not
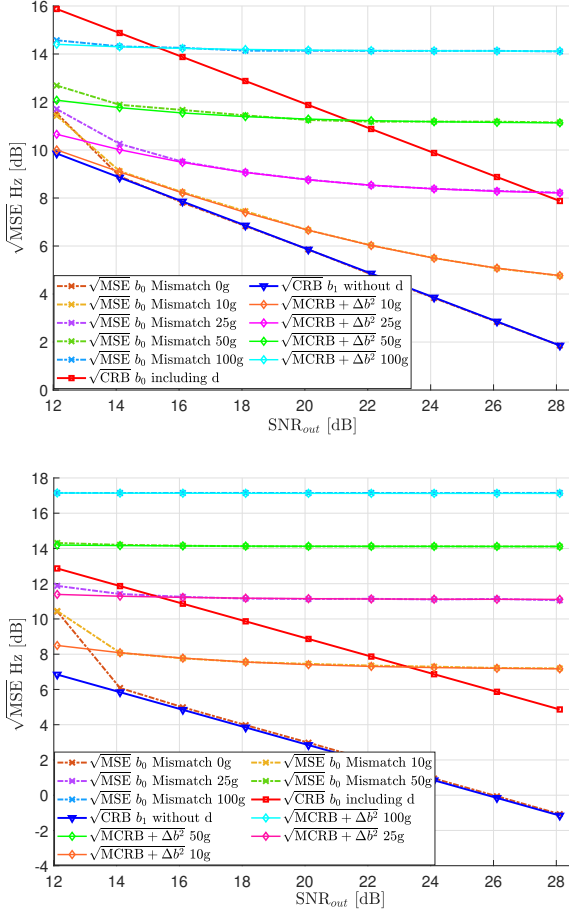
Fig. 5. Doppler CRB and MSE mismatch for 10 ms F_s = 2.046 MHz (Top) and 20 ms F_s = 1.023 MHz (Bottom)
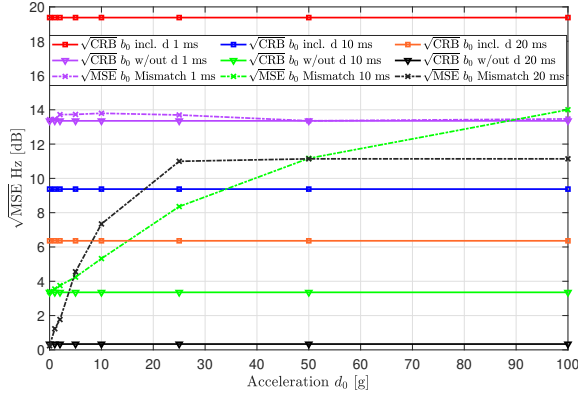

Fig. 6. Doppler CRB and MSE mismatch for 1 ms, 10 ms, and 20 ms for different magnitudes of acceleration

able to cause a significant enough change in the Doppler to degrade the performance of the mismatch MLE. For the higher duration (20 ms), the increase is steeper, quickly exceeding the delay/Doppler/acceleration CRB, and eventually settles to some value below the bound for the 1 ms delay/Doppler CRB_b. Through trial and error, this value was found to be approximately equal to the delay/Doppler/acceleration bound for

TABLE I
ACCELERATION THRESHOLD VALUES FOR SNR= 25dB IN THE GPS C/A SYSTEM

Estimation duration	Optimum mismatch error	Threshold for acceleration estimation
1 ms	a > 90g (better than 10 ms)	Never
10 ms	5g < a < 50g	≈ 35g
20 ms	a < 5g, a > 50g	≈ 9g

a signal length of 6 ms. This means that for high magnitude accelerations, the minimum period of 6ms is needed for the fully specified estimator to perform better than the mismatch MLE. Table I gives a summary of the key thresholds determined from Figure 6. These are approximations since the resolution of the different acceleration calculations is not optimized. The results in Table I give an estimation of the magnitude of acceleration that the GPS C/A system must be reached for the delay/Doppler/acceleration MLE to be necessary for optimizing Doppler estimation, a threshold for high dynamics. Conversely, it also gives the limit of low acceleration values for which the biased mismatch MLE is preferred (although not attaining the CRB). An interesting result is a threshold for 20 ms being 9g, this value is close to the limit allowable for manned vehicles [34]. So it can be concluded that for optimum Doppler estimation of a fast-moving manned vehicle e.g. a launch vehicle or crew capsule, the mismatch MLE is the ideal choice for estimation. For any vehicles accelerating with a greater magnitude e.g. ballistics missiles, it is preferred to use the delay/Doppler/acceleration MLE (for any duration longer than 6 ms). Note that this analysis is specific for SNR = 25 dB, the magnitudes may differ for different operating conditions. For general scenarios, accelerations greater than 30g require the inclusion of acceleration estimation to optimize the error in the Doppler (and this general threshold value is lower for higher SNR scenarios).

Finally, we assess the impact on the acceleration estimation in Figures 7 and 8. The mismatched acceleration estimate is obtained from a linear regression (LR) using consecutive Doppler estimates. As was seen above, the error in the Doppler mismatch estimate depends on the magnitude of acceleration and so the LR calculation will also have performance losses. Since the total duration of signal observation is 20 ms, the bound to compare is the 20 ms CRB_d. Four different scenarios for the LR calculation are used for analysis. Figure 7 (top) shows the performance of 4 consecutive 5 ms estimates, and Figure 7 (bottom) uses 2 consecutive 10 ms estimates. The remaining cases are the inverses (5x4 ms and 10x2 ms) and are displayed in Figure 8. The LR error in Figure 7 (top) does not reach the CRB for 20 ms because of the higher magnitude of error for each 5 ms Doppler estimate. Therefore, the LR-based acceleration estimation error seems to increase for high dynamics and short consecutive estimation periods. Figure 7 also shows that the LR mismatch error flattens out

at lower SNR values as the acceleration increases (see 75g and 100g). For lower magnitude accelerations, it is preferred to use longer observation times as the added error due to neglecting acceleration is not as significant for the LR model. The trade-off between acceleration and observation intervals for the mismatch LR error at a representative SNR = 25 dB is shown in Figure 8. The preferred length of consecutive Doppler estimates is 2×10 ms. These results further confirm that for high magnitude accelerations, it is preferred to not neglect the acceleration term.
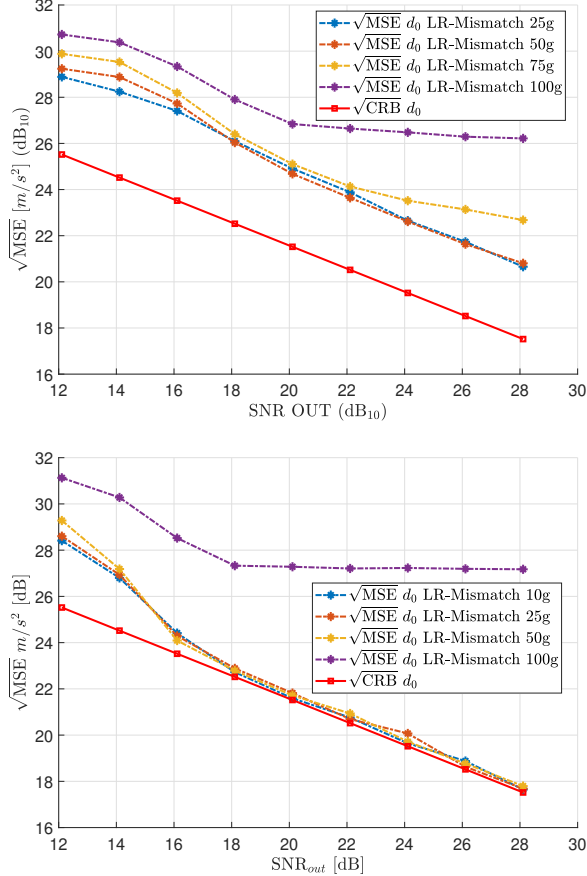

Fig. 7. Acceleration CRB and MSE LR mismatch for consecutive Doppler estimates of 4x5 ms (Top) and 2x10 ms (Bottom)

B. Radar LFM Chirp Signal Scenario

To further support the discussion, in the sequel we present a second example to assess the validity of the new CRB expressions. We consider a radar LFM chirp signal classically defined as,

$$s(t) = e^{j2\pi f(t)}, \ f(t) = \frac{B}{2T}\left(\frac{t}{T} - \frac{1}{2}\right)^2, \ T = NT_s, \qquad (28)$$

with B the chirp bandwidth equal to 2 MHz and N the number of samples. Moreover, we consider a signal duration of 10 ms and F_s = 2.046 MHz. To synthesize a high dynamics scenario we consider again the previous set of parameters where the Doppler is equal to 10 kHz and acceleration is equal to 100g. In Figures 9 and 10, we illustrate the new
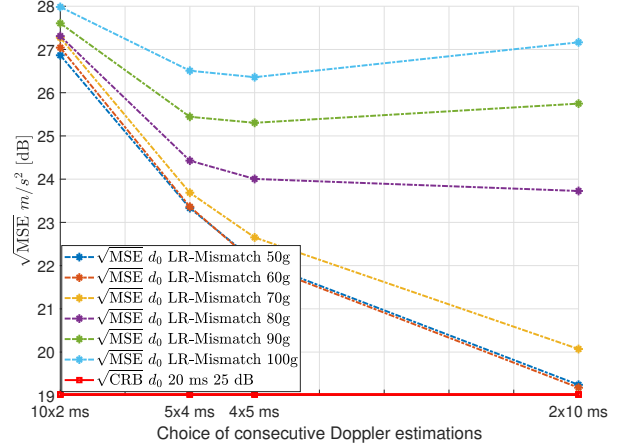

Fig. 8. Trade-off for a number of consecutive Doppler estimation periods to optimize acceleration mismatch error (SNR = 25 dB)

CRBs and the corresponding MLE for the set of parameters $\boldsymbol{\eta} = [\tau, b, d]^{\top}$ in terms of SNR$_{out}$, obtained for 1000 Monte Carlo runs. From Figure 9, we confirm again that the delay estimation is not affected by the acceleration term for 10 ms, and both MLE τ_0 and MLE τ_0 "Mismatch" coincide. In Figure 10 (top plot) we show the results for the Doppler estimation considering 1 ms and 10 ms of a signal. Note that as in the GPS C/A signal example, for 1 ms of signal we can see that the Doppler estimate converges to the corresponding CRB, with or without acceleration. Moreover, adding the acceleration parameter degrades the CRB around 6 dB. In contrast, when considering 10 ms of signal, the MLE accounting for the acceleration converges to the CRB whereas the mismatched Doppler MLE does not. The MLE mismatch does not converge in this case, compared to the 1 ms observation time because the duration of the signal gives enough time for the Doppler to change significantly due to acceleration. The estimated value of Doppler is therefore the expected value for zero acceleration and is biased by the amount of shift due to acceleration. Again, we conclude that if the Doppler cannot be assumed constant during the observation time, the acceleration must be considered to obtain a correct estimate (for high magnitude accelerations). Finally, we assess the acceleration estimation performance in Figure 10 (bottom plot). The mismatched acceleration is computed from an LR using 10 consecutive 1 ms Doppler estimates. Note that while the acceleration MLE converges to the corresponding CRB, the LR-based acceleration leads to an important loss of performance.

VI. CONCLUSION

In this contribution, we derived novel CRB compact form expressions for the joint delay, Doppler, and acceleration estimation. These expressions are valid for a generic band-limited signal, avoiding the standard narrowband assumption, and therefore can be exploited in several applications. The new CRB expressions have the advantage that they have been derived by using a baseband signal model that is defined on sampled versions of the signals. This inherently accounts for
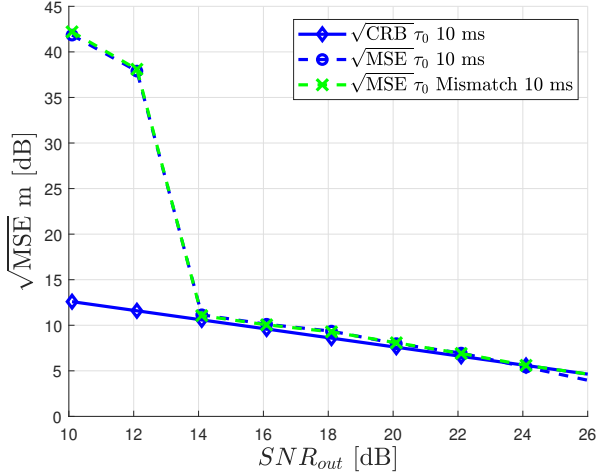
Fig. 9. Delay CRB/MSE for F_s = 2.046 MHz and 10 ms of a Radar LFM chirp signal.
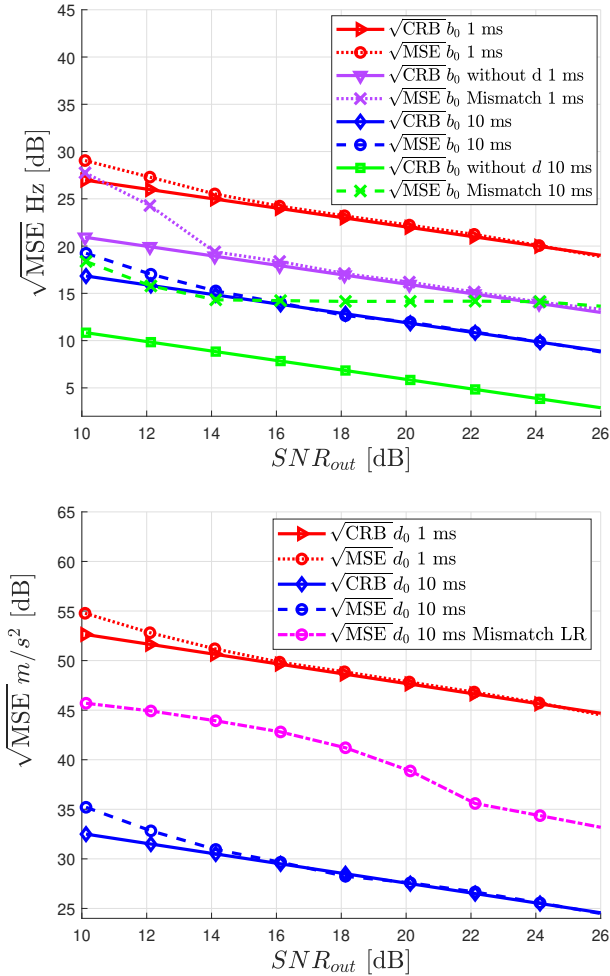

Fig. 10. Doppler (Top) and Acceleration (Bottom) CRB/MSE of Radar LFM chirp signal for F_s = 2.046 MHz duration 1 ms and 10 ms.

the effect of the sampling frequency and a limited number of samples in the observation time. Results were illustrated using representative GPS L1 C/A and LFM chirp band-limited signals. The validity of the new CRBs was demonstrated by resorting to the MLE and the ambiguity function. Both results confirmed the validity and exactness of the proposed CRBs. To complete the discussion, the performance loss of conventional delay/Doppler approaches in high dynamics scenarios, w.r.t. delay/Doppler/acceleration results were also shown for both signals. A range of high dynamics acceleration values have been determined, which indicate when the MLE including acceleration is the preferred choice over the mismatched delay/Doppler MLE.

APPENDIX A

A. Details on the CRB Derivation

Recall that $\beta = 1 - b$, $\omega_c = 2\pi f_c$, $s^{(1)}(t) = \frac{ds(t)}{dt}$ and $s^{(2)}(t) = \frac{d^2 s(t)}{dt^2}$. We search to derive a compact form of $\text{Re}\{\boldsymbol{\Phi}(\boldsymbol{\eta})\}$, which can be rewritten as

$$\text{Re}\{\boldsymbol{\Phi}(\boldsymbol{\eta})\} = \text{Re}\left\{\frac{\partial \mathbf{a}(\boldsymbol{\eta})^H}{\partial \boldsymbol{\eta}^T} \frac{\partial \mathbf{a}(\boldsymbol{\eta})}{\partial \boldsymbol{\eta}^T}\right\}$$
$$- \text{Re}\left\{-\frac{1}{\|\mathbf{a}(\boldsymbol{\eta})\|^2}\left(\mathbf{a}(\boldsymbol{\eta})^H \frac{\partial \mathbf{a}(\boldsymbol{\eta})}{\partial \boldsymbol{\eta}^T}\right)^H \left(\mathbf{a}(\boldsymbol{\eta})^H \frac{\partial \mathbf{a}(\boldsymbol{\eta})}{\partial \boldsymbol{\eta}^T}\right)\right\},$$

where the vector $\frac{\partial \boldsymbol{a}(\boldsymbol{\eta})}{\partial \boldsymbol{\eta}} = \left[\begin{array}{ccc} \frac{\partial \boldsymbol{a}(\boldsymbol{\eta})}{\partial \tau} & \frac{\partial \boldsymbol{a}(\boldsymbol{\eta})}{\partial b} & \frac{\partial \boldsymbol{a}(\boldsymbol{\eta})}{\partial d} \end{array}\right]^T$ is

$$-\begin{bmatrix} (1-b)s^{(1)}(t;\boldsymbol{\eta}) - (j\omega_c b + j2\omega_c d(t-\tau))s(t;\boldsymbol{\eta}) \\ (t-\tau)s^{(1)}(t;\boldsymbol{\eta}) + j\omega_c(t-\tau)s(t;\boldsymbol{\eta}) \\ j\omega_c(t-\tau)^2 s(t;\boldsymbol{\eta}) \end{bmatrix}$$
$$\times e^{-j\omega_c(b(t-\tau)+d(t-\tau)^2)},$$

and it can be expressed in terms of the following matrices,

$$\frac{\partial \mathbf{a}(t;\boldsymbol{\eta})}{\partial \boldsymbol{\eta}} = -\mathbf{Q}\boldsymbol{\vartheta}e^{-j\omega_c(b(t-\tau)+d(t-\tau)^2)}, \quad (29)$$

$$Q = \begin{bmatrix} -j\omega_c b & -j2\omega_c d & (1-b) & 0 & 0 \\ 0 & j\omega_c & 0 & 0 & 1 \\ 0 & 0 & 0 & j\omega_c & 0 \end{bmatrix}, \quad (30)$$

$$\boldsymbol{\vartheta} = \begin{bmatrix} s(t;\boldsymbol{\eta}) \\ (t-\tau)s(t;\boldsymbol{\eta}) \\ s^{(1)}(t;\boldsymbol{\eta}) \\ (t-\tau)^2 s(t;\boldsymbol{\eta}) \\ (t-\tau)s^{(1)}(t;\boldsymbol{\eta}) \end{bmatrix}. \quad (31)$$

Representing the signal with discrete time values ($t = kT_s$ and $N_1 \leq k \leq N_2$) allows the products to be expressed as sums,

$$\|\mathbf{a}(\boldsymbol{\eta})\|^2 = \sum_{k=N_1}^{N_2} |s(kT_s;\boldsymbol{\eta})|^2, \quad (32)$$

$$\mathbf{a}(\boldsymbol{\eta})^H \frac{\partial \mathbf{a}(\boldsymbol{\eta})}{\partial \boldsymbol{\eta}^T} = -\left(\sum_{k=N_1}^{N_2} \boldsymbol{\vartheta}(kT_s;\boldsymbol{\eta})s^*(kT_s;\boldsymbol{\eta})\right)^T \mathbf{Q}^T, \quad (33)$$

$$\frac{\partial \mathbf{a}(\boldsymbol{\eta})^H}{\partial \boldsymbol{\eta}^T} \frac{\partial \mathbf{a}(\boldsymbol{\eta})}{\partial \boldsymbol{\eta}^T} = \mathbf{Q}^* \left(\sum_{k=N_1}^{N_2} \boldsymbol{\vartheta}^*(kT_s;\boldsymbol{\eta})\boldsymbol{\vartheta}^T(kT_s;\boldsymbol{\eta})\right) \mathbf{Q}^T. \quad (34)$$

Taking $s(t)$ as a band-limited signal, and using the Nyquist-Shannon theorem, we have that

$$\lim_{\substack{N1\to-\infty\\N2\to\infty}} \text{Re}\left\{\boldsymbol{\Phi}(\boldsymbol{\eta})\right\} = F_s\text{Re}\left\{\mathbf{QWQ}^H - \frac{(\mathbf{Qw})(\mathbf{Qw})^H}{w_1}\right\}, \quad (35)$$

where $\mathbf{w} = \begin{bmatrix} w_1 \\ w_2 \\ w_3 \\ w_4 \\ w_5 \end{bmatrix}$ and $\mathbf{W} = \begin{bmatrix} w_1 & w_2^* & w_3^* & w_4^* & w_5^* \\ w_2 & W_{2,2} & W_{3,2}^* & W_{4,2}^* & W_{5,2}^* \\ w_3 & W_{3,2} & W_{3,3} & W_{4,3}^* & W_{5,3}^* \\ w_4 & W_{4,2} & W_{4,3} & W_{4,4} & W_{5,4}^* \\ w_5 & W_{5,2} & W_{5,3} & W_{5,4} & W_{5,5} \end{bmatrix}$,

and the different terms are expressed from the baseband signal samples as

$$w_1 = \int_{-\infty}^{\infty} |s(t;\boldsymbol{\eta})|^2\, dt = \frac{1}{\beta F_s}\mathbf{s}^H\mathbf{s},$$

$$w_2 = \int_{-\infty}^{\infty} (t-\tau)\,|s(t;\boldsymbol{\eta})|^2\, dt = \frac{1}{\beta^2 F_s^2}\mathbf{s}^H\mathbf{Ds},$$

$$w_3 = \int_{-\infty}^{\infty} s^{(1)}(t;\boldsymbol{\eta})s(t;\boldsymbol{\eta})dt = \frac{1}{\beta}\mathbf{s}^H\boldsymbol{\Lambda}\mathbf{s},$$

$$w_4 = W_{2,2} = \int_{-\infty}^{\infty} (t-\tau)^2\,|s(t;\boldsymbol{\eta})|^2\, dt = \frac{1}{\beta^3 F_s^3}\mathbf{s}^H\mathbf{D}^2\mathbf{s},$$

$$w_5 = W_{3,2} = \int_{-\infty}^{\infty} (t-\tau)s^{(1)}(t;\boldsymbol{\eta})s^*(t;\boldsymbol{\eta})dt = \frac{1}{\beta^2 F_s}\mathbf{s}^H\mathbf{D}\boldsymbol{\Lambda}\mathbf{s},$$

$$W_{3,3} = \int_{-\infty}^{\infty} \left|s^{(1)}(t;\boldsymbol{\eta})\right|^2\, dt = \frac{F_s}{\beta}\mathbf{s}^H\mathbf{Vs},$$

$$W_{4,2} = \int_{-\infty}^{\infty} (t-\tau)^3\,|s(t;\boldsymbol{\eta})|^2\, dt = \frac{1}{\beta^4 F_s^4}\mathbf{s}^H\mathbf{D}^3\mathbf{s},$$

$$W_{4,3} = W_{5,2} = \int_{-\infty}^{\infty} (t-\tau)^2 s^{(1)}(t;\boldsymbol{\eta})s^*(t;\boldsymbol{\eta})dt$$

$$= \frac{1}{\beta^3 F_s^2}\left(\mathbf{s}^H\mathbf{D}\boldsymbol{\Lambda}\mathbf{Ds} - \mathbf{s}^H\mathbf{Ds}\right),$$

$$W_{4,4} = \int_{-\infty}^{\infty} (t-\tau)^4\,|s(t;\boldsymbol{\eta})|^2\, dt = \frac{1}{\beta^5 F_s^5}\mathbf{s}^H\mathbf{D}^4\mathbf{s},$$

$$W_{5,3} = \int_{-\infty}^{\infty} \left|s^{(1)}(t;\boldsymbol{\eta})\right|^2\, dt = \frac{1}{\beta^2}\left(\mathbf{s}^H\boldsymbol{\Lambda}\mathbf{s} + \mathbf{s}^H\mathbf{VDs}\right),$$

$$W_{5,4} = \int_{-\infty}^{\infty} (t-\tau)^3 s^{(1)}(t;\boldsymbol{\eta})s^*(t;\boldsymbol{\eta})dt$$

$$= \frac{1}{\beta^4 F_s^3}\left(\mathbf{s}^H\mathbf{D}\boldsymbol{\Lambda}\mathbf{D}^2\mathbf{s} - \mathbf{s}^H\mathbf{D}^2\mathbf{s}\right),$$

$$W_{5,5} = \int_{-\infty}^{\infty} \left|s^{(1)}(t;\boldsymbol{\eta})\right|^2\, dt$$

$$= \frac{1}{\beta^3 F_s}\left(\mathbf{s}^H\mathbf{s} + \mathbf{Ds}^H\mathbf{VDs} - 2Re\left\{\mathbf{s}^H\mathbf{VDs}\right\}\right).$$

B. Further Details on the Computation of $\mathbf{W}$

Because the computation of the inner terms in $\mathbf{W}$ from the baseband signal samples is not straightforward, we give the details for three terms (i.e., $W_{4,2}$, $W_{4,4}$ and $W_{5,4}$). Notice that the rest of the terms were computed for the delay/Doppler CRB in [24]. Let us recall that if $s(t) \rightleftharpoons s(f)$, then $ts(t) \rightleftharpoons \frac{j}{2\pi}s^{(1)}(f)$, $t^2 s(t) \rightleftharpoons -\frac{1}{4\pi^2}s^{(2)}(f)$ and $ts^{(1)}(t) \rightleftharpoons -s(f) - fs^{(1)}(f)$. Moreover, we have the following mathematical equivalences, which allow to operate with the signal samples,

$$s(f) = \frac{1}{F_s}\sum_{N_1}^{N_2} s(nT_s)e^{-j2\pi\frac{f}{F_s}n}, \quad (36)$$

$$s^{(1)}(f) = \frac{-j2\pi}{F_s^2}\sum_{N_1}^{N_2} ns(nT_s)e^{-j2\pi\frac{f}{F_s}n}, \quad (37)$$

$$s^{(2)}(f) = \frac{-4\pi^2}{F_s^3}\sum_{N_1}^{N_2} n^2 s(nT_s)e^{-j2\pi\frac{f}{F_s}n}. \quad (38)$$

The terms $W_{4,2}$, $W_{4,4}$ and $W_{5,4}$ are derived as follows:

$$W_{4,2} = \int_{-\infty}^{\infty}(t-\tau)^3\,|s(t;\boldsymbol{\eta})|^2\, dt = \frac{1}{\beta^4}\int_{-\infty}^{\infty} t^3\,|s(t)|^2\, dt$$

$$= \frac{1}{\beta^4}\int_{-\infty}^{\infty}(t^2 s(t))(ts(t))^*\, dt$$

$$\rightleftharpoons \frac{1}{\beta^4}\int_{-\frac{F_s}{2}}^{\frac{F_s}{2}} -\frac{1}{4\pi^2}s^{(2)}(f)\left(\frac{j}{2\pi}s^{(1)}(f)\right)^*\, df = \frac{1}{\beta^4 F_s^4}\mathbf{s}^H\mathbf{D}^3\mathbf{s},$$

$$W_{4,4} = \int_{-\infty}^{\infty}(t-\tau)^4\,|s(t;\boldsymbol{\eta})|^2\, dt = \frac{1}{\beta^5}\int_{-\infty}^{\infty} t^4\,|s(t)|^2\, dt$$

$$= \frac{1}{\beta^5}\int_{-\infty}^{\infty}(t^2 s(t))(t^2 s(t))^*\, dt$$

$$\rightleftharpoons \frac{1}{\beta^5}\int_{-\frac{F_s}{2}}^{\frac{F_s}{2}} -\frac{1}{4\pi^2}s^{(2)}(f)\left(-\frac{1}{4\pi^2}s^{(2)}(f)\right)^*\, df = \frac{1}{\beta^5 F_s^5}\mathbf{s}^H\mathbf{D}^4\mathbf{s},$$

$$W_{5,4} = \int_{-\infty}^{\infty}(t-\tau)^3 s^{(1)}(t;\boldsymbol{\eta})s(t;\boldsymbol{\eta})dt$$

$$= \frac{1}{\beta^4}\int_{-\infty}^{\infty} t^3 s^{(1)}(t)s^*(t)dt = \frac{1}{\beta^4}\int_{-\infty}^{\infty}\left(ts^{(1)}(t)\right)\left(t^2 s^*(t)\right)dt$$

$$\rightleftharpoons \frac{1}{\beta^4}\int_{-\frac{F_s}{2}}^{\frac{F_s}{2}}\left(-s(f) - fs^{(1)}(f)\right)\left(\frac{-1}{4\pi^2}s^{(2)}(f)\right)^*\, df$$

$$= \frac{1}{\beta^4}\int_{-\frac{F_s}{2}}^{\frac{F_s}{2}}\frac{1}{4\pi^2}s(f)\left(s^{(2)}(f)\right)^*\, df$$

$$+ \frac{1}{\beta^4}\int_{-\frac{F_s}{2}}^{\frac{F_s}{2}}\frac{1}{4\pi^2}fs^{(1)}(f)\left(s^{(2)}(f)\right)^*\, df$$

$$= \frac{1}{\beta^4 F_s^3}\left(\mathbf{s}^H\mathbf{D}\boldsymbol{\Lambda}\mathbf{D}^2\mathbf{s} - \mathbf{s}^H\mathbf{D}^2\mathbf{s}\right).$$

C. Compact form Expression of $\text{Re}\left\{\boldsymbol{\Phi}(\boldsymbol{\eta})\right\}$

To obtain the compact form expression in terms of $\mathbf{W}$, we need to compute the terms $\mathbf{QWQ}^H$ and $\frac{(\mathbf{Qw})(\mathbf{Qw})^H}{w_1}$ in (35),

$$\left(\mathbf{QWQ}^H\right)_{1,1} = \begin{pmatrix} 4\omega_c^2 bd\text{Re}\{w_2\} - 4\omega_c d(1-b)\text{Im}\{W_{3,2}\} \\ +(\omega_c b)^2 w_1 - 2\omega_c b(1-b)\text{Im}\{w_3\} \\ +4\omega_c^2 d^2 W_{2,2} + (1-b)^2 W_{3,3} \end{pmatrix},$$

$$\left(\mathbf{QWQ}^H\right)_{1,2} = \begin{pmatrix} -\omega_c^2 bw_2^* - 2\omega_c^2 dW_{2,2} - j\omega_c bw_5^* \\ -j\omega_c 2dW_{5,2}^* + (1-b)(-j\omega_c W_{3,2} + W_{5,3}^*) \end{pmatrix},$$

$$\left(\mathbf{QWQ}^H\right)_{1,3} = -\omega_c^2 bw_4^* - 2\omega_c^2 dW_{4,2}^* - j\omega_c(1-b)W_{4,3}^*,$$

$$\left(\mathbf{QWQ}^H\right)_{2,2} = \omega_c^2 W_{2,2} + 2\omega_c\text{Im}\{W_{5,2}\} + W_{5,5},$$

$$\left(\mathbf{QWQ}^H\right)_{2,3} = \omega_c^2 W_{4,2}^* - j\omega_c W_{5,4},$$

$$\left(\mathbf{Q}\mathbf{W}\mathbf{Q}^H\right)_{3,3} = \omega_c^2 W_{4,4}, \tag{39}$$

and

$$\left(\frac{(\mathbf{Qw})(\mathbf{Qw})^H}{w_1}\right)_{1,1} = \begin{pmatrix} (\omega_c b)^2 w_1 + 4\omega_c^2 bd(1-b)\mathrm{Re}\{w_2\} \\ -2\omega_c b(1-b)\mathrm{Im}\{w_3\} + 4\omega_c^2 d^2 \frac{|w_2|^2}{w_1} \\ -4\omega_c(1-b)d\mathrm{Im}\left\{\frac{w_2^* w_3}{w_1}\right\} \\ +(1-b)^2\frac{|w_3|^2}{w_1} \end{pmatrix},$$

$$\left(\frac{(\mathbf{Qw})(\mathbf{Qw})^H}{w_1}\right)_{1,2} = \begin{pmatrix} -\omega_c^2 bw_2^* - 2\omega_c^2 d\frac{|w_2|^2}{w_1} \\ -j\omega_c(1-b)\frac{w_2^* w_3}{w_1} + (1-b)\frac{w_5^* w_3}{w_1} \\ -j\omega_c bw_5^* + j\omega_c 2d\frac{w_5^* w_2}{w_1} \end{pmatrix},$$

$$\left(\frac{(\mathbf{Qw})(\mathbf{Qw})^H}{w_1}\right)_{1,3} = \begin{pmatrix} -\omega_c^2 bw_4^* - 2\omega_c^2 d\frac{w_2 w_4^*}{w_1} \\ -j\omega_c(1-b)\frac{w_4^* w_3}{w_1} \end{pmatrix},$$

$$\left(\frac{(\mathbf{Qw})(\mathbf{Qw})^H}{w_1}\right)_{2,2} = \omega_c^2\frac{|w_2|^2}{w_1} + \frac{|w_5|^2}{w_1} + 2\omega_c\mathrm{Im}\left\{\frac{w_2 w_5}{w_1}\right\},$$

$$\left(\frac{(\mathbf{Qw})(\mathbf{Qw})^H}{w_1}\right)_{2,3} = \omega_c^2\frac{w_2 w_4^*}{w_1} - j\omega_c\frac{w_5 w_4^*}{w_1},$$

$$\left(\frac{(\mathbf{Qw})(\mathbf{Qw})^H}{w_1}\right)_{3,3} = \omega_c^2\frac{|w_4|^2}{w_1}. \tag{40}$$

Finally, injecting (39) and (40) into (35), leads to the expression in (19).

D. Details on the Standard Narrowband Signal Model CRB

If the impact of the Doppler and acceleration parameters in the received baseband signal is negligible, $s(t - \tau_0(t)) \simeq s(t - \tau)$. Then, $a(t; \boldsymbol{\eta}) = e^{-j2\pi f_c(b(t-\tau)+d(t-\tau)^2)}s(t-\tau)$, and

$$\frac{\partial \mathbf{a}(t; \boldsymbol{\eta})}{\partial \boldsymbol{\eta}} = -\mathbf{Q}\boldsymbol{\vartheta}e^{-j\omega_c(b(t-\tau)+d(t-\tau)^2)}, \tag{41}$$

with

$$\mathbf{Q} = \begin{bmatrix} -j\omega_c b & -j2\omega d & 1 & 0 \\ 0 & j\omega_c & 0 & 0 \\ 0 & 0 & 0 & j\omega_c \end{bmatrix}, \boldsymbol{\vartheta} = \begin{bmatrix} s(t; \boldsymbol{\eta}) \\ (t-\tau)s(t; \boldsymbol{\eta}) \\ s^{(1)}(t; \boldsymbol{\eta}) \\ (t-\tau)^2 s(t; \boldsymbol{\eta}) \end{bmatrix}.$$

Again, $\mathrm{Re}\{\boldsymbol{\Phi}(\boldsymbol{\eta})\}$ can be expressed as in (35), with $\mathbf{w}$ and $\mathbf{W}$ given now by

$$\mathbf{w} = [w_1, w_2, w_3, w_4]^\top \text{ and } \mathbf{W} = \begin{bmatrix} w_1 & w_2^* & w_3^* & w_4^* \\ w_2 & W_{2,2} & W_{3,2}^* & W_{4,2}^* \\ w_3 & W_{3,2} & W_{3,3} & W_{4,3}^* \\ w_4 & W_{4,2} & W_{4,3} & W_{4,4} \end{bmatrix}.$$

Following the same procedure than for the wideband signal case, we can compute $\mathbf{Q}\mathbf{W}\mathbf{Q}^H$ and $\frac{(\mathbf{Qw})(\mathbf{Qw})^H}{w_1}$, which injected into (35) lead to the narrowband CRB expressions in (25).

REFERENCES

[1] H. L. Van Trees, *Detection, Estimation, and Modulation Theory, Part III: Radar – Sonar Signal Processing and Gaussian Signals in Noise.* John Wiley & Sons, 2001.

[2] ——, *Optimum Array Processing.* Wiley-Interscience, New-York, 2002.

[3] P. J. G. Teunissen and O. Montenbruck, Eds., *Handbook of Global Navigation Satellite Systems.* Switzerland: Springer, 2017.

[4] V. U. Zavorotny, S. Gleason, E. Cardellach, and A. Camps, "Tutorial on Remote Sensing using GNSS Bistatic Radar of Opportunity," *IEEE Geosci. Remote Sens. Mag.*, vol. 2, no. 4, pp. 8–45, Dec. 2014.

[5] V. Chen, Fayin Li, Shen-Shyang Ho, and H. Wechsler, "Micro-doppler effect in radar: phenomenon, model, and simulation study," *IEEE Transactions on Aerospace and Electronic Systems*, vol. 42, no. 1, pp. 2–21, Jan. 2006. [Online]. Available: http://ieeexplore.ieee.org/document/1603402/

[6] H. L. Van Trees, K. L. Bell, and Z. Tian, *Detection, Estimation and Modulation Theory - Part 1*, 2nd ed. Wiley, 2013.

[7] P. Stoica and A. Nehorai, "Performances Study of Conditional and Unconditional Direction of Arrival Estimation," *IEEE Trans. Acoust., Speech, Signal Process.*, vol. 38, no. 10, pp. 1783–1795, Oct. 1990.

[8] A. Renaux, P. Forster, E. Chaumette, and P. Larzabal, "On the High-SNR Conditional Maximum-Likelihood Estimator Full Statistical Characterization," *IEEE Trans. Signal Process.*, vol. 54, no. 12, pp. 4840 – 4843, Dec. 2006.

[9] P. Closas, C. Fernández-Prades, and J. A. Fernández-Rubio, "Cramér-Rao Bound Analysis of Positioning Approaches in GNSS Receivers," *IEEE Trans. on Signal Processing*, vol. 57, no. 10, pp. 3775–3786, Nov. 2009.

[10] D. Medina, L. Ortega, J. Vilà-Valls, P. Closas, F. Vincent, and E. Chaumette, "Compact CRB for Delay, Doppler and Phase Estimation - Application to GNSS SPP & RTK Performance Characterization," *IET Radar, Sonar & Navigation*, vol. 14, no. 10, pp. 1537–1549, Sep. 2020.

[11] A. Dogandzic and A. Nehorai, "Cramér-Rao Bounds for Estimating Range, Velocity, and Direction with an Active Array," *IEEE Trans. Signal Process.*, vol. 49, no. 6, pp. 1122–1137, June 2001.

[12] Y. Chen and R. S. Blum, "On the Impact of Unknown Signals on Delay, Doppler, Amplitude, and Phase Parameter Estimation," *IEEE Trans. Signal Process.*, vol. 67, no. 2, pp. 431–443, Jan. 2019.

[13] D. Medina, J. Vilà-Valls, E. Chaumette, F. Vincent, and P. Closas, "Cramér-Rao Bound for a Mixture of Real- and Integer-valued Parameter Vectors and its Application to the Linear Regression Model," *Signal Processing*, vol. 179, p. 107792, Feb. 2021.

[14] W. Huang, M. M. Naghsh, R. Lin, and J. Li, "Doppler Sensitive Discrete-Phase Sequence Set Design for MIMO Radar," *IEEE Transactions on Aerospace and Electronic Systems*, vol. 56, no. 6, pp. 4209–4223, Dec. 2020. [Online]. Available: https://ieeexplore.ieee.org/document/9093027/

[15] A. W. Rihaczek, "Delay-Doppler Ambiguity Function for Wideband Signals," *IEEE Trans. Aerosp. Electron. Syst.*, vol. 3, no. 4, pp. 705–711, July 1967.

[16] D. A. Swick, "A Review of Wideband Ambiguity Functions," Naval Res. Lab., Washington DC, Tech. Rep. 6994, 1969.

[17] D. W. Ricker, *Echo Signal Processing.* Springer, New York, USA: Kluwer Academic, 2003.

[18] Q. Jin, K. M. Wong, and Z.-Q. Luo, "The Estimation of Time Delay and Doppler Stretch of Wideband Signals," *IEEE Trans. Signal Process.*, vol. 43, no. 4, p. 904–916, April 1995.

[19] X. Niu, P. C. Ching, and Y. Chan, "Wavelet Based Approach for Joint Time Delay and Doppler Stretch Measurements," *IEEE Trans. Aerosp. Electron. Syst.*, vol. 35, no. 3, pp. 1111–1119, July 1999.

[20] W. He-Wen, Y. Shangfu, and W. Qun, "Influence of Random Carrier Phase on True Cramér-Rao Lower Bound for Time Delay Estimation," in *Proc. of the ICASSP*, Honolulu, USA, April 2007.

[21] Z. Nan, T. Zhao, and T. Huang, "Cramér-Rao Lower Bounds of Joint Time Delay and Doppler-stretch Estimation with Random Stepped-frequency Signals," in *Proc. of the IEEE DSP*, Beijing, China, October 2016.

[22] T. Zhao and T. Huang, "Cramér-Rao Lower Bounds for the Joint Delay-Doppler Estimation of an Extended Target," *IEEE Trans. Signal Process.*, vol. 64, no. 6, pp. 1562–1573, March 2016.

[23] I. Gogolev and G. Yashin, "Cramér-Rao Lower Bound of Doppler Stretch and Delay in Wideband Signal Model," in *Proc. of the IEEE Conf. of Russian Young Researchers in EEE (EIConRus)*, St. Petersburg, Russia, April 2017.

[24] P. Das, J. Vilà-Valls, F. Vincent, L. Davain, and E. Chaumette, "A New Compact Delay, Doppler Stretch and Phase Estimation CRB with a Band-Limited Signal for Generic Remote Sensing Applications," *Remote Sensing*, vol. 12, no. 18, p. 2913, Sep. 2020.

[25] S. Fortunati, F. Gini, M. S. Greco, and C. D. Richmond, "Performance Bounds for Parameter Estimation under Misspecified Models: Fundamental Findings and Applications," *IEEE Signal Processing Magazine*, vol. 34, no. 6, pp. 142–157, Nov. 2017.

[26] P. D. Groves, *Principles of GNSS, Inertial, and Multisensor Integrated Navigation Systems*, 2nd ed. Artech House, 2013.

[27] Y. J. Morton, F. Van Diggelen, J. J. Spilker, and B. W. Parkinson, Eds., *Position, Navigation, and Timing Technologies in the 21st Century:*

Integrated Satellite Navigation, Sensor Systems, and Civil Applications. New Jersey, USA: Wiley-IEEE Press, 2021.

[28] L. Ortega, J. Vilà-Valls, and E. Chaumette, "Insights on the Estimation Performance of GNSS-R Coherent and Non-Coherent Processing Schemes," *IEEE Geoscience and Remote Sensing Letters, early access*, 2022.

[29] M. I. Skolnik, *Radar Handbook*, 3rd ed. New York, USA: McGraw-Hill, 1990.

[30] E. J. Kelly, "The Radar Measurement of Range, Velocity and Acceleration," *IRE Transactions on Military Electronics*, no. 2, pp. 51–57, 1961.

[31] J. Chen, Y. Huang, and J. Benesty, "Time delay estimation," in *Audio Signal Processing for Next-Generation Multimedia Communication Systems*, Y. Huang and J. Benesty, Eds. Boston, MA, USA: Springer, 2004, ch. 8, pp. 197–227.

[32] B. Ottersten, M. Viberg, P. Stoica, and A. Nehorai, "Exact and Large Sample Maximum Likelihood Techniques for Parameter Estimation and Detection in Array Processing," in *Radar Array Processing*, S. Haykin, J. Litva, and T. J. Shepherd, Eds. Heidelberg: Springer-Verlag, 1993, ch. 4, pp. 99–151.

[33] A. Mennad, S. Fortunati, M. N. El Korso, A. Younsi, A. M. Zoubir, and A. Renaux, "Slepian-Bangs-type formulas and the related Misspecified Cramér-Rao Bounds for Complex Elliptically Symmetric distributions," *Signal Processing*, vol. 142, pp. 320–329, 2018. [Online]. Available: https://hal.parisnanterre.fr//hal-01654607

[34] C. Lawrence, E. L. Fasanella, A. Tabiei, J. W. Brinkley, and D. M. Shemwell, "The Use of a Vehicle Acceleration Exposure Limit Model and a Finite Element Crash Test Dummy Model to Evaluate the Risk of Injuries During Orion Crew Module Landings," Apr. 2008. [Online]. Available: https://ntrs.nasa.gov/api/citations/20080018587/downloads/20080018587.pdf